Supporting Information

Table S1 Kinetics model fitting parameters for Cd(II) uptaken by three Fe-nanomaterials (Experimental conditions: initial Cd(II) = 10 mg/L, material dose = 20 mg/L, t = 3 h).

Material	pH	$q_{e,exp}$ (mg/g)	Pseudo-first-order			Pseudo-second-order		
			k_1 (1/min)	q_e (mg/g)	R^2	k_2 (g/(mg·min))	q_e (mg/g)	R^2
nZVI	4	85.75				0.0020[a)]	59.88	0.6152
	6	102.50				0.0062[a)]	104.17	0.9947
	8	122.50				0.0023[a)]	117.65	0.9772
S-nZVI	4	436.30	0.0076	17.31	0.1054	0.0023	434.78	0.9992
	6	467.50	0.0164	189.28	0.9062	0.0004	454.55	0.9985
	8	475.60	0.0152	224.23	0.9272	0.0003	476.19	0.9990
nFeS	4	358.75	0.0207	24.22	0.8641	0.0024	370.37	0.9997
	6	445.59	0.0216	59.53	0.9505	0.0024	434.78	0.9998
	8	470.40	0.0129	52.82	0.6536	0.0020	476.19	0.9999

Notes: a) the Cd(II) release of nZVI was found to begin at ~ 90 min, thus, the value k_2 of nZVI was calculated at 90 min.

Table S2 Changes of the XPS Fe 2p peaks of the samples before and after reaction.

Material	Situation	Species	Binding energy	FWHM
Nzvi	before reaction	Fe^0	707.24	1.46
		Fe(II)-O	710.96	3.00
		Fe(III)-O	713.25	4.86
		satellite	719.50	2.92
		Fe(III)-O	724.87	4.70
	after reaction	Fe(II)-O	711.28	2.85
		Fe(III)-O	713.56	3.43
		satellite	719.10	4.03
		Fe(III)-O	725.15	4.08
S-Nzvi	before reaction	Fe^0	707.64	1.67
		Fe(II)-O/Fe(II)-S	711.12	3.13
		Fe(III)-O	713.85	2.95
		satellite	719.65	3.09
		Fe(III)-O	724.72	4.25
	after reaction	Fe(II)-O/Fe(II)-S	711.50	2.70
		Fe(III)-O	713.46	3.60
		satellite	719.70	3.83
		Fe(III)-O	725.50	4.03
NFeS	before reaction	Fe(II)-O/Fe(II)-S	710.79	3.69
		Fe(III)-O	712.20	5.50
		satellite	719.70	5.56
		Fe(III)-O	724.82	4.65
	after reaction	Fe(II)-O/Fe(II)-S	710.73	4.53
		Fe(III)-O	713.20	5.50
		satellite	718.60	6.00
		Fe(III)-O	725.00	5.50

Table S3 Changes of the XPS S 2p peaks of the samples before and after reaction.

Material	Situation	Species	Binding energy	FWHM
S-Nzvi	before reaction	surface S^{2-}	161.02	1.02
		bulk S^{2-}	162.12	1.56
		S_n^{2-}	163.55	2.77
	after reaction	bulk S^{2-}	161.67	1.15
		S_n^{2-}	162.84	1.64
NFeS	before reaction	surface S^{2-}	160.66	0.97
		bulk S^{2-}	161.60	1.30
		S_n^{2-}	163.10	2.10
	after reaction	bulk S^{2-}	161.43	0.97
		S_n^{2-}	162.53	1.70

Table S4 Changes of the XPS Cd 3p peaks of the samples before and after reaction.

Material	Situation	Species	Binding energy	FWHM
Nzvi	after reaction	Cd(II)	405.70	1.51
		Cd(II)	412.45	1.50
S-Nzvi	after reaction	Cd(II)	405.48	1.37
		Cd(II)	412.24	1.44
NFeS	after reaction	Cd(II)	405.28	1.15
		Cd(II)	412.02	1.14

Table S5 Changes of the XPS O 1s peaks of the samples before and after reaction.

Material	Situation	Species	Binding energy	FWHM
Nzvi	before reaction	O^{2-}	530.06	1.10
		-OH	531.51	2.49
	after reaction	-OH	531.48	2.72
S-Nzvi	before reaction	O^{2-}	530.01	1.30
		-OH	531.74	2.20
	after reaction	-OH	531.44	2.94
NFeS	before reaction	O^{2-}	529.48	1.10
		-OH	531.03	2.13
	after reaction	O^{2-}	530.14	1.03
		-OH	532.04	2.00

Table S6 Cd(II) removal capacity by various materials.

Material	pH_0	Initial dose (mg/L)	Initial $C_{Cd(II)}$ (mg/L)	q_E (mg/g)	Ref.
nZVI	5	500	10	42.5	(Su et al., 2015)
nZVI	8.6	5000	50	66.9	(Zhang et al., 2014)
FeS	6	5000	30	13.4	(Mustafa et al., 2010)
CMC-FeS	6	100	1	398.3	(Tian et al., 2020)
S-nZVI	5	500	20	85.0	(Su et al., 2015)
S-nZVI	7	300	20	150.0	(Lv et al., 2018)
S-nZVI	6	300	200	495.0	(Liang et al., 2020)
nZVI	6	20	10	102.5	This work
S-nZVI	6	20	10	467.5	This work
FeS	6	20	10	445.6	This work

Table S7 The pseudo-first-order and pseudo-second-order kinetic model fitting parameters for Fe(II) release by three Fe-nanomaterials (Experimental conditions: initial Cd(II) = 10 mg/L, material dose = 20 mg/L, *t* = 3 h).

Material	pH	$c_{eFe,\ exp}$ (mg/L)	Pseudo-first-order			Pseudo-second-order		
			$k_{1Fe(II)}$ (1/min)	c_{eFe} (mg/L)	R^2	$k_{2Fe(II)}$ (L/(mg·min))	c_{eFe} (mg/L)	R^2
nZVI	4	2.21	0.0051	0.27	0.3919	0.1997	2.17	0.9963
	6	0.75	0.0025	0.37	0.5448	0.9918	0.49	0.9659
	8	1.02	0.0078	0.39	0.7173	0.0991	1.00	0.9709
S-nZVI	4	5.32	0.0036	0.29	0.0164	0.2098	5.22	0.9996
	6	3.29	0.0225	1.99	0.9593	0.0328	3.38	0.9954
	8	2.83	0.0062	1.64	0.8337	0.0890	2.05	0.9986
nFeS	4	4.27	0.0441	0.75	0.8508	0.3071	4.27	0.9999
	6	2.52	0.0099	0.17	0.5549	0.3726	2.51	0.9995
	8	2.17	0.0096	0.25	0.2742	24.8423	2.06	0.9978

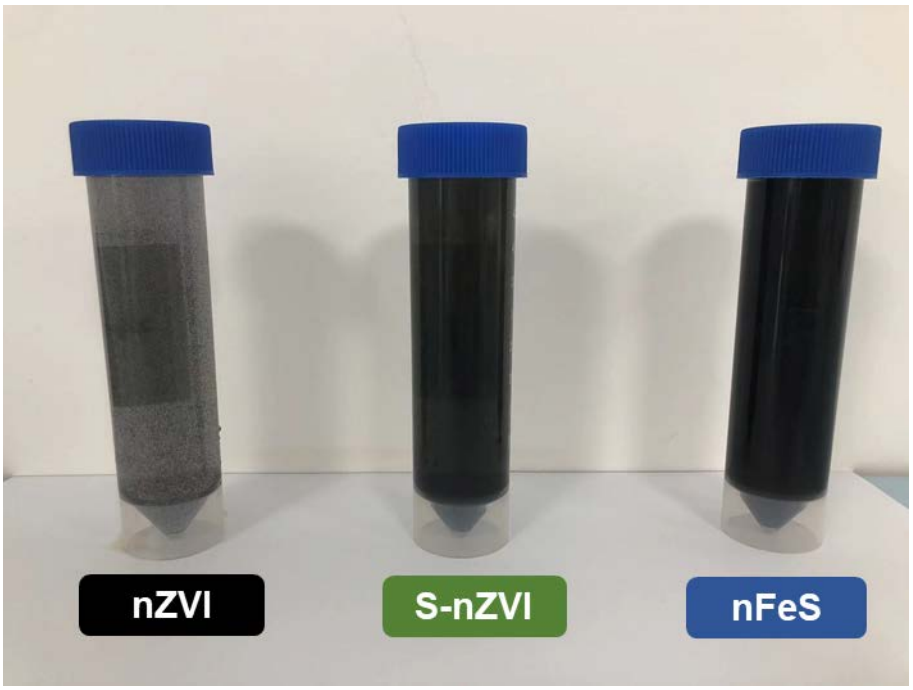

Fig. S1 Photo of three Fe-based materials (material dose = 100 mg/L).

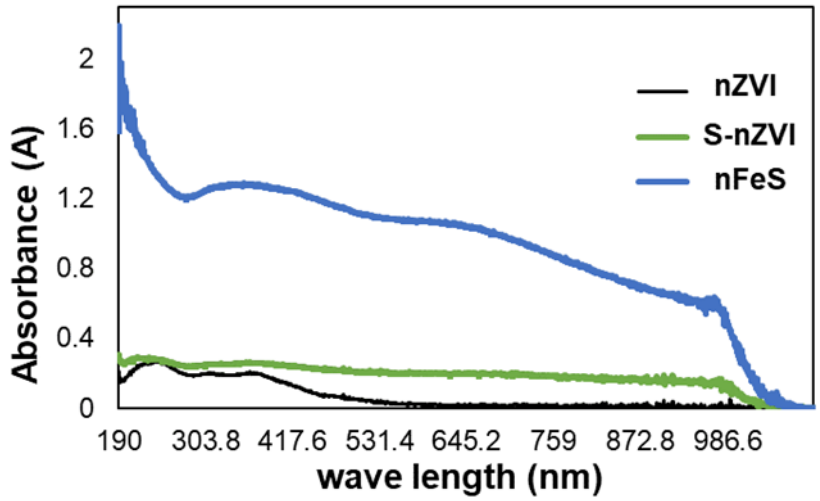

Fig. S2 UV-Vis spectrum of three Fe-based materials (material dose = 20 mg/L).

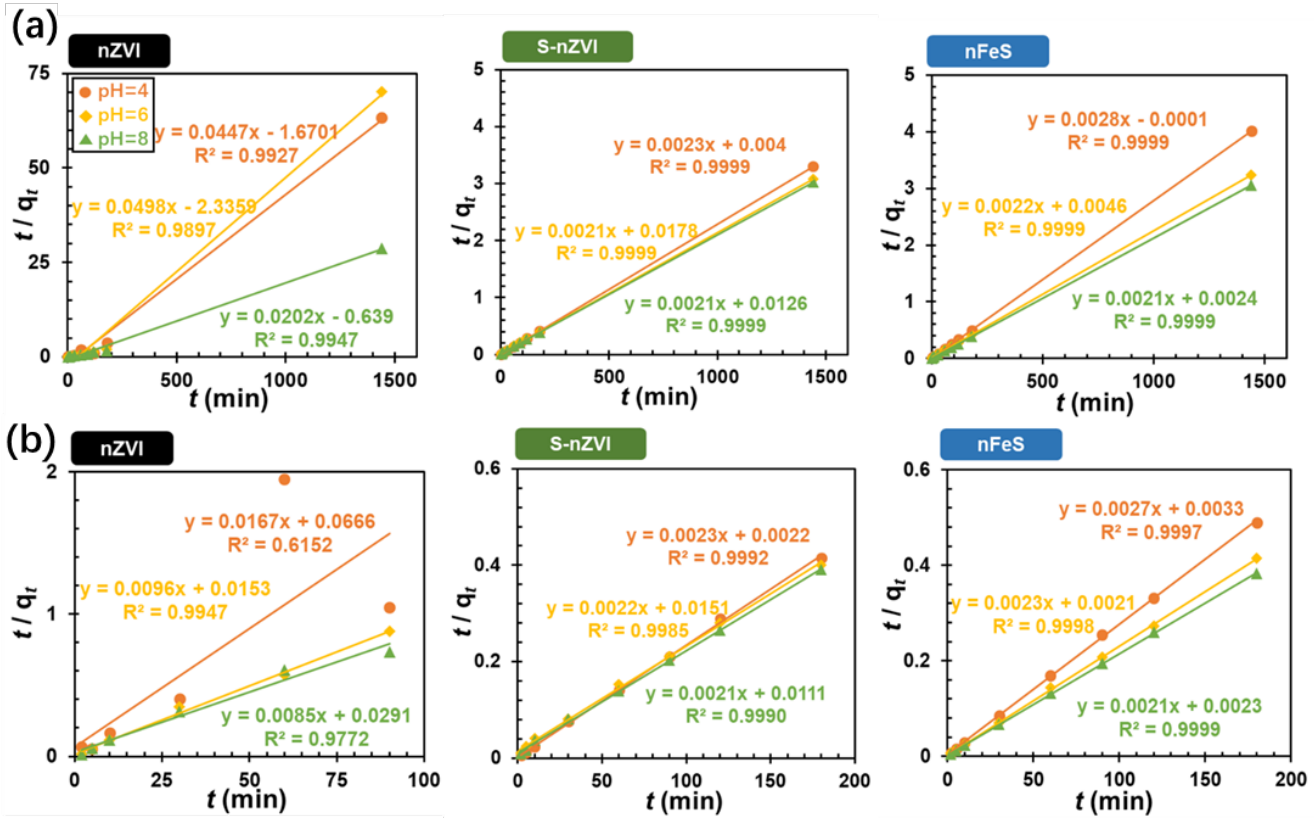

Fig. S3 Pseudo-second-order kinetic modelling of three Fe-based nanomaterials under different pH: **(a)** 24 h, **(b)** 3 h (Experimental conditions: initial Cd(II) = 10 mg/L, material dose = 20 mg/L. The Cd(II) release of nZVI (b) was found to begin at ~ 90 min, thus, pseudo-second-order kinetic modelling of nZVI was calculated from 0 to 90 min).

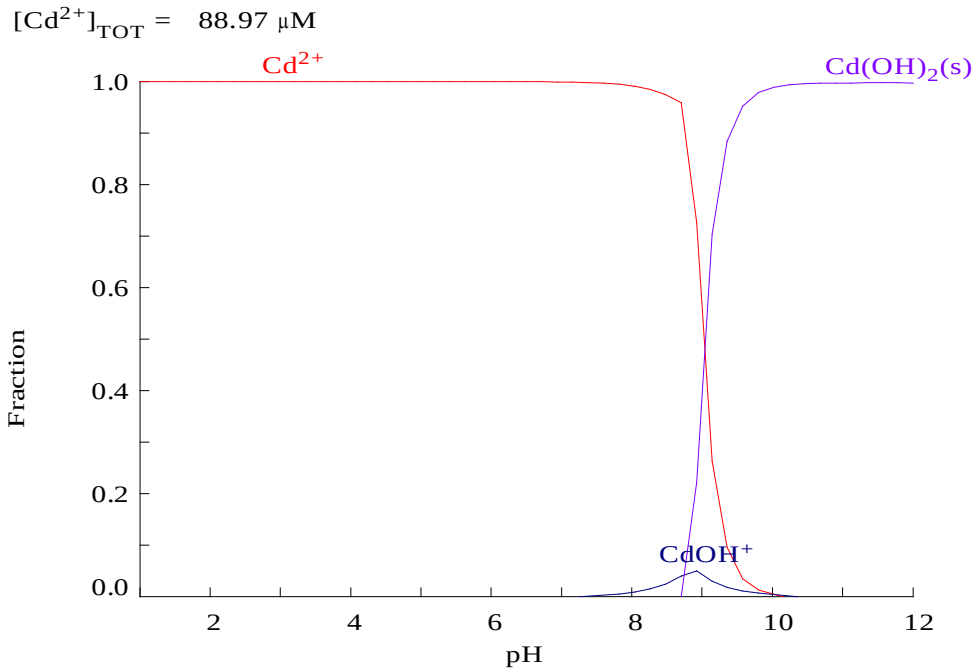

Fig. S4 Cd(II) species distribution as calculated per Medusa 2014 (developed by Ignasi Puigdomenech of KTH, Sweden).

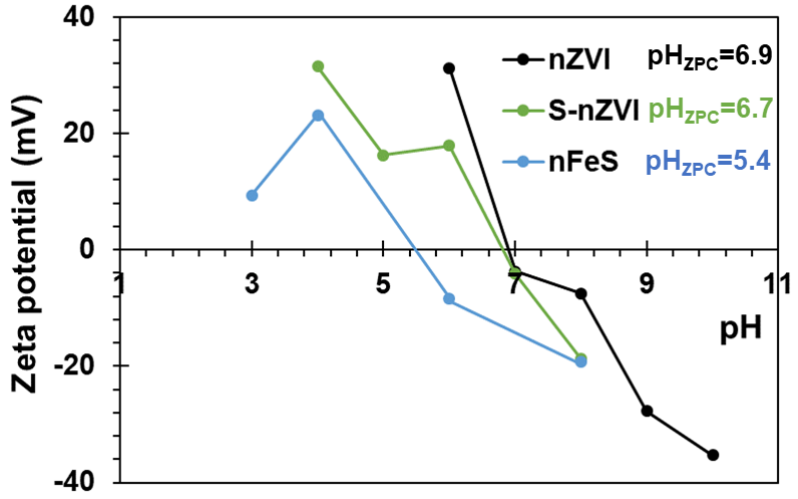

Fig. S5 Zeta potential of three materials as a function of pH.

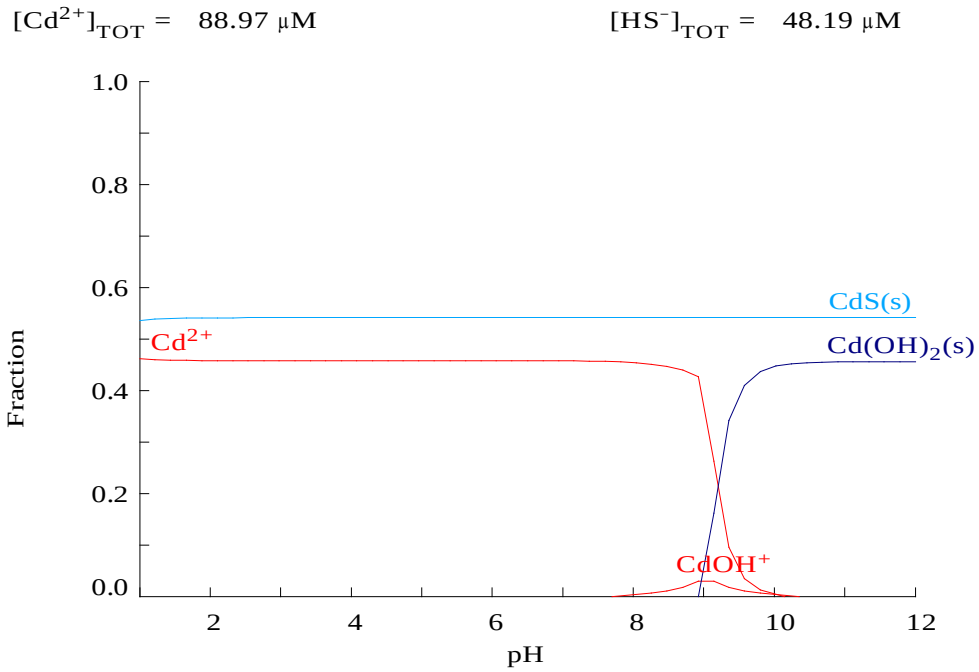

Fig. S6 Cd(II) species distribution with the presence of HS- as calculated per Medusa 2014 (developed by Ignasi Puigdomenech of KTH, Sweden).

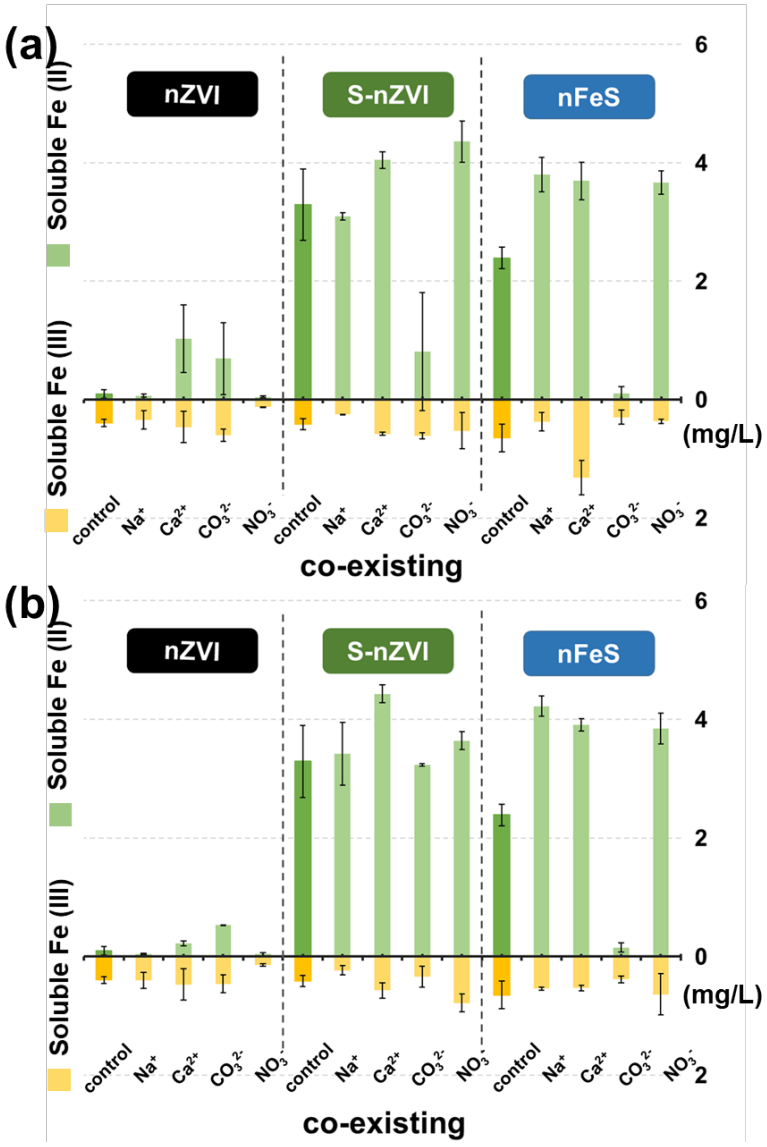

Fig. S7 The dissolution of Fe under different concentrations of co-existing **(a)** 50 mg/L, **(b)** 200 mg/L (Experimental conditions: initial Cd(II) = 10 mg/L, initial pH = 6.0, material dose = 20 mg/L, *t* = 24 h).

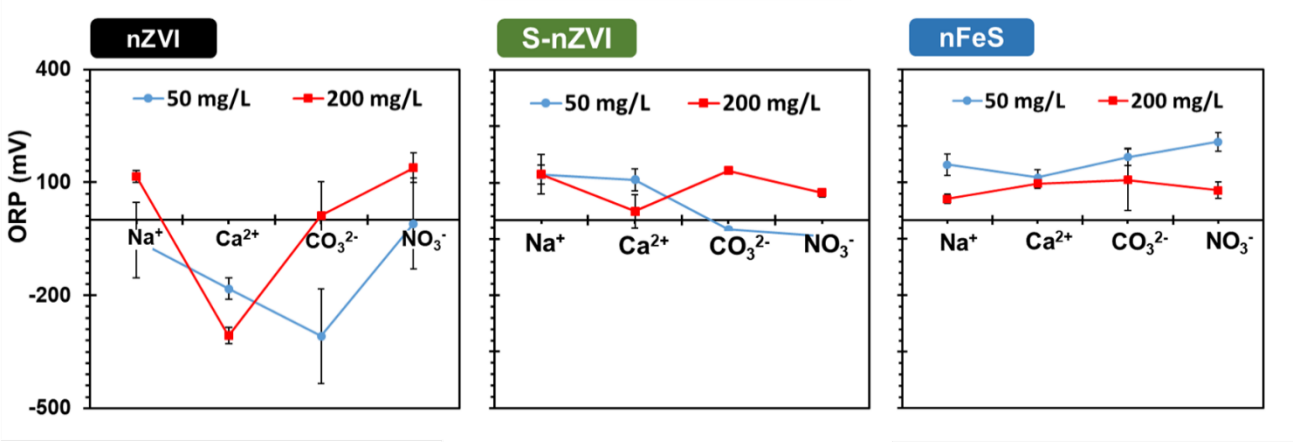

Fig. S8 Final values of ORP in the different co-existing solutions (Experimental conditions: initial Cd(II) = 10 mg/L, initial pH = 6.0, material dose = 20 mg/L, *t* = 24 h).

$[Cd^{2+}]_{TOT}$ = 88.97 μM

$[Fe^{2+}]_{TOT}$ = 38.24 μM

$[CO_3^{2-}]_{TOT}$ = 0.83 mM

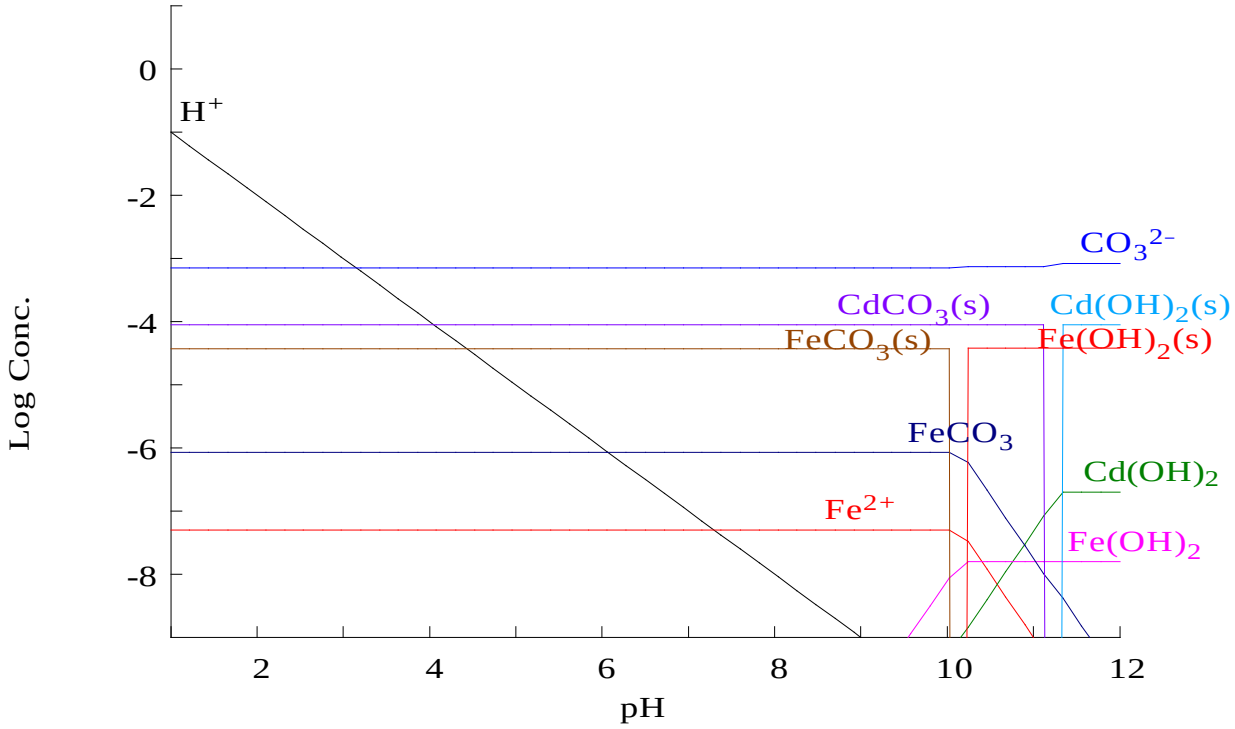

Fig. S9 Cd(II) and Fe(II) species distribution with the presence of CO_3^{2-}.

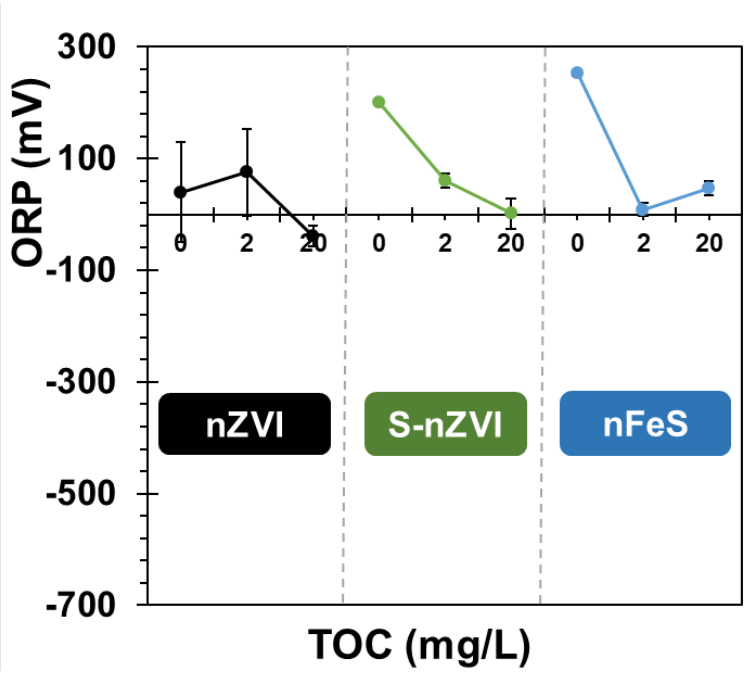

Fig. S10 Final values of ORP with the presence of different concentrations of HA.

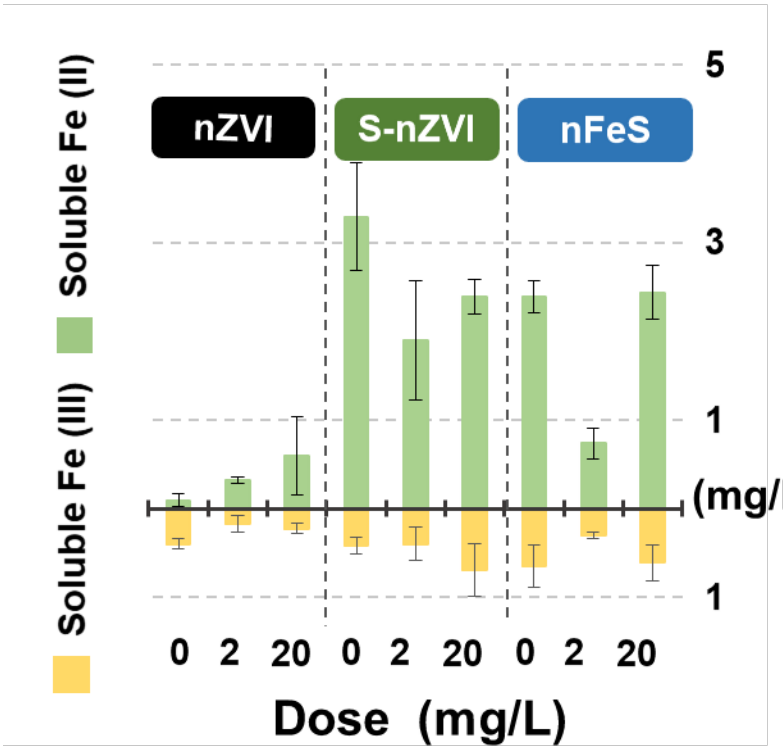

Fig. S11 The dissolution of Fe under the different dose of TOC.

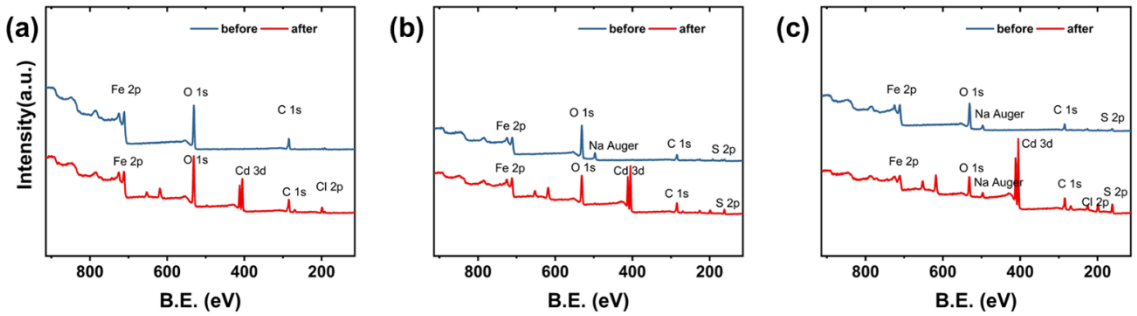

Fig. S12 XPS broad survey of **(a)** nZVI, **(b)** S-nZVI, and **(c)** nFeS.

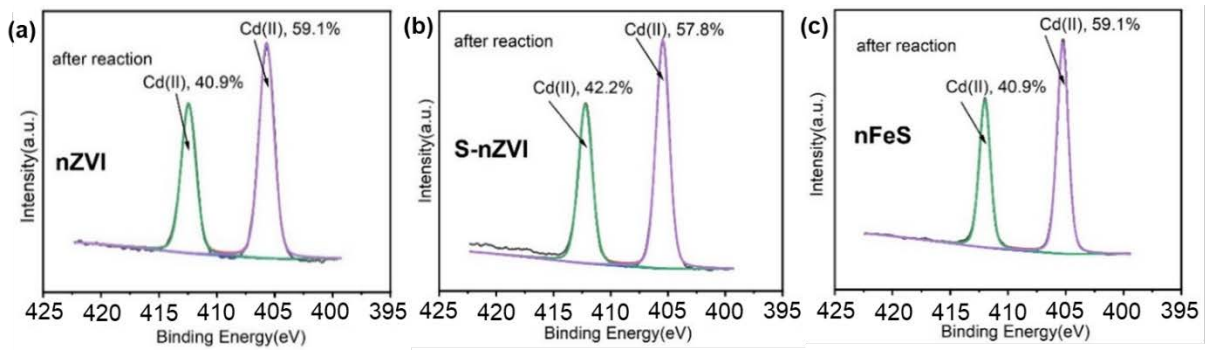

Fig. S13 Cd 3d XPS spectra of **(a)** nZVI, **(b)** S-nZVI, and **(c)** nFeS.

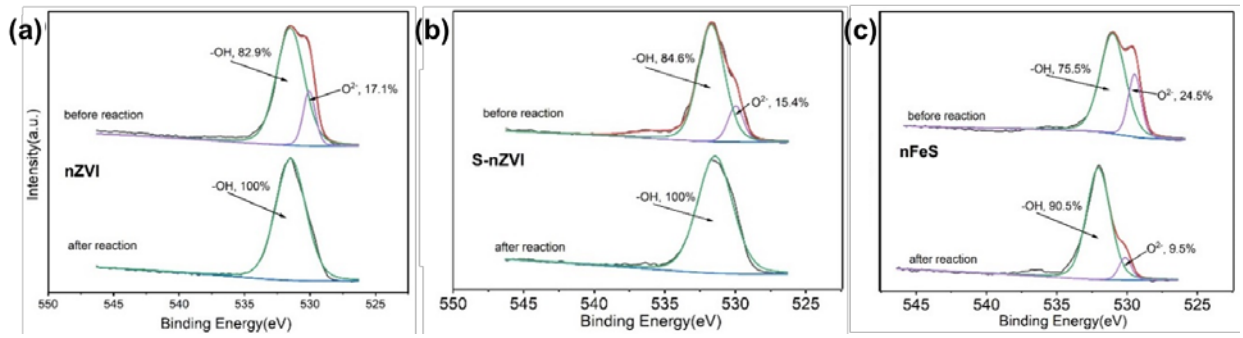

Fig. S14 O 1s XPS spectrum of **(a)** nZVI, **(b)** S-nZVI, and **(c)** nFeS.

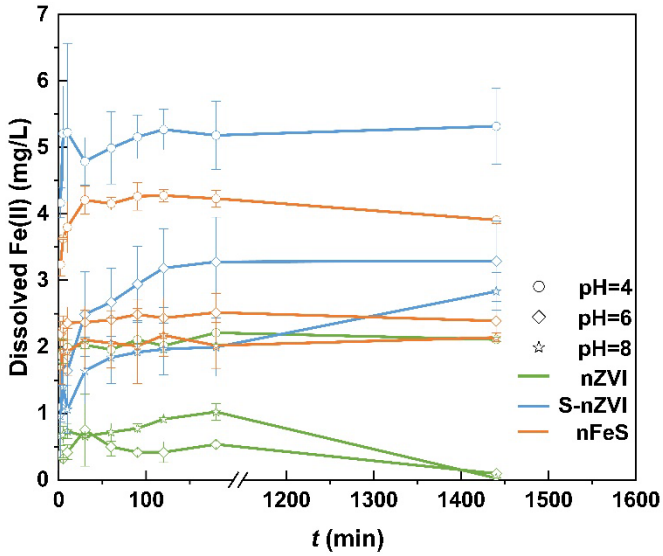

Fig. S15 The variation of dissolved Fe(II) with time in three nanomaterials at pH = 4, 6, and 8.

References

Liang L, Li X, Lin Z, Tian C, Guo Y (2020). The removal of Cd by sulfidated nanoscale zero-valent iron: the structural, chemical bonding evolution and the reaction kinetics. Chemical Engineering Journal, 382: 122933

Lv D, Zhou X, Zhou J, Liu Y, Li Y, Yang K, Lou Z, Baig S A, Wu D, Xu X (2018). Design and characterization of sulfide-modified nanoscale zerovalent iron for cadmium(II) removal from aqueous solutions. Applied Surface Science, 442: 114–123

Mustafa S, Misbahud D, Sammad Y H, Zaman M I, Sadullah K (2010). Sorption mechanism of cadmium from aqueous solution on iron sulphide. Chinese Journal of Chemistry, 28(7): 1153–1158

Su Y, Adeleye A S, Keller A A, Huang Y, Dai C, Zhou X, Zhang Y (2015). Magnetic sulfide-modified nanoscale zerovalent iron (S-nZVI) for dissolved metal ion removal. Water Research, 74: 47–57

Tian S, Gong Y, Ji H, Duan J, Zhao D (2020). Efficient removal and long-term sequestration of cadmium from aqueous solution using ferrous sulfide nanoparticles: performance, mechanisms, and long-term stability. Science of The Total Environment, 704: 135402

Zhang Y, Li Y, Dai C, Zhou X, Zhang W (2014). Sequestration of Cd(II) with nanoscale zero-valent iron (nZVI): characterization and test in a two-stage system. Chemical Engineering Journal, 244: 218–226

26